



WIND FLOW MODEL PERFORMANCE

Do more sophisticated models produce more accurate wind resource estimates?

Philippe Beaucage, Research Scientist

Michael C. Brower, Chief Technical Officer

February 6, 2012



INTRODUCTION

The optimal design of a wind project and the accurate prediction of its energy production depend on having an accurate and detailed understanding of the spatial distribution of the wind resource across the project area. Nowadays, numerical wind flow modeling, combined with onsite meteorological measurements, is the preferred approach to estimate this distribution. It is consequently important to continually assess potential improvements in numerical wind flow models.

Linear wind flow models like WASP (Troen 1990) are widely used to predict the spatial variation of the average wind speed, directional frequency distribution (wind rose), wind shear, and other boundary layer characteristics. Most such models are based on the theory of Jackson and Hunt (1975). They came into wide use in the 1980s when the computing resource was very limited. They run fast while performing reasonably well where the wind is not significantly affected by steep slopes, flow separations, thermally driven flows, low-level jets, and other dynamic and nonlinear phenomena.

Computational Fluid Dynamics (CFD) models are considered the next generation of wind flow models for wind energy applications. Most CFD models solve the mass and momentum conservation components of the non-linear Navier-Stokes equations, and are run until convergence is reached using a constant inlet wind profile. For idealized cases, i.e. 2D or 3D flow over escarpments and hills, such steady-state CFD models perform well and give a high level of detail on the turbulence characteristics of the flow (Biatsuamlak et al. 2004). Several research studies show that CFD models perform better than the industry standard WASP model in many but not all cases (Berge et al., 2006, Periera et al. 2010, VanLuvanee et al. 2009, Sumner et al., 2010).

On the next rung up the ladder of sophistication are mesoscale numerical weather prediction (NWP) models (e.g., MASS, WRF, ARPS, MC2, KAMM, etc.). In principle, fully compressible, non-hydrostatic NWP models can simulate and capture a broad range of meteorological phenomena from synoptic to micro scales, but the required computing power is substantial and increases rapidly with decreasing grid spacing. To circumvent this issue, NWP models are usually coupled with linear “microscale” wind flow models to achieve a high spatial resolution. The microscale models used for this purpose include Jackson-Hunt-type models (e.g., WASP, MsMicro (Taylor et al. 1983), Raptor (Ayotte and Taylor 1995)) and mass-conserving models (e.g. WindMap (Brower 1999), CALMET (Scire et al. 2000)). Two leading examples of such coupled mesoscale-microscale models are the KAMM/WASP system developed by Risoe National Laboratory (Frank and Landberg, 1997) and the SiteWind system developed by AWS Truepower (Brower, 1999). AWS Truepower’s approach is to run the mesoscale model (MASS) for a sample of days in nested grids down to a resolution of 400 m to 1.2 km. Then, the mean wind flow is downscaled to approximately 50-m grid spacing using the microscale model (WindMap). Previous research has suggested that this approach is more accurate than the industry-standard WASP model over wind-project-scale distances in complex terrain, especially where mesoscale circulations have a significant impact on the spatial distribution of the wind resource (Reed et al., 2004).

The next level of sophistication is NWP models coupled to large-eddy simulations (LES). LES models have their origin in meteorology and weather prediction (Deardorff 1972, Moeng 1984, Mason 1994) and solve the unsteady, non-linear Navier-Stokes equations with the full physics parameterization schemes (radiation, microphysics, cloud convection, land surface-atmosphere interaction, turbulence, etc.). They are run at a high resolution compared to NWP models, i.e. close to an inertial sub-range of 3D turbulence, and are therefore able to explicitly resolve the energetically important eddies of the flow while parameterizing the small ones. The validity of LES depends crucially on the quality of the chosen turbulence closure scheme because of limited grid resolution and thermal stratification effects. However, LES models are mainly used as a research tool since the necessary computing power represents a major hurdle.

The present study aims to characterize the mean wind flow at four different sites with different mesoscale circulations and surface characteristics. One of the sites is in flat terrain, one in a coastal area and two in mountainous terrain. Five different numerical wind flow models are compared:

- WASP - a linear Jackson-Hunt wind flow model
- Meteodyn WT - a CFD model
- WindMap/openWind® Enterprise - a mass-consistent model

- SiteWind® - a coupled mesoscale NWP-mass-consistent model
- ARPS - a coupled mesoscale NWP-LES

METHODOLOGY

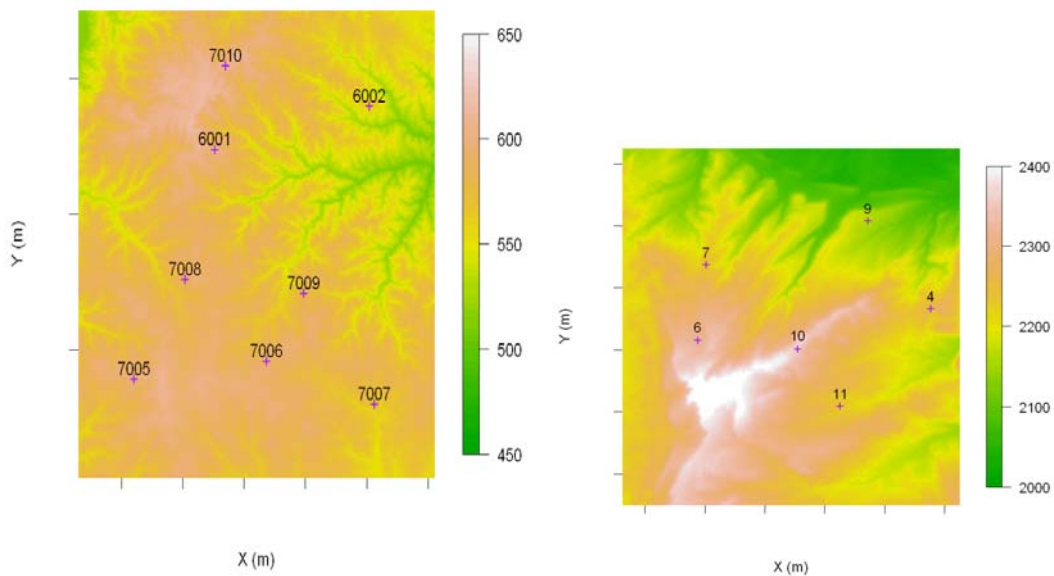
Figure 1 shows the terrain elevation and met mast locations for the four sites in this study. Site 1 is located in the US Great Plains and is fairly flat with a mix of grassland and trees. Site 2 is in a mountainous region of the Western US and has a homogeneous grassland ground cover. Site 3 is located near one of the Great Lakes in Canada and is forested. Site 4 is in the Gaspé Peninsula in Canada and is also forested. These sites were chosen because of the diversity of conditions they represent, the number of met masts installed, and the quality of the data. The RIX values at the met masts range around 0%, 0-3%, 0-1% and 0-8% for site 1 through 4, respectively.

Mass-consistent model

The WindMap model is based on the NOABL objective analysis code (Phillips 1979, Sherman 1978). The model was further improved to take into account internal boundary layer growth due to sharp transition in surface roughness (Brower 1999). This mass-consistent model contains no dynamic equations. It solves the conservation of mass equation to generate a 3-D, terrain-dependent, divergence-free wind flow. The WindMap model is initialized using surface and upper-air wind data when run in conjunction with a NWP model or using met mast data when run in openWind.

Linear Jackson-Hunt wind flow model

The Wind Atlas Analysis and Application Program (WAsP) developed at Risoe DTU National Laboratory is a spectral model based on the Jackson-Hunt theory. The model solves the linearized Navier-Stokes equations under several assumptions: steady-state flow, linear advection, and first-order turbulence closure. In addition, the terrain is only taken into account as a first-order perturbation. In order to improve the accuracy of the predictions, some analysts apply statistical corrections based on a terrain roughness index (RIX) (Mortensen 2008). For comparability with the other wind flow models, however, no such correction is applied here. For this study, WAsP is run with a 50-m grid cell spacing.



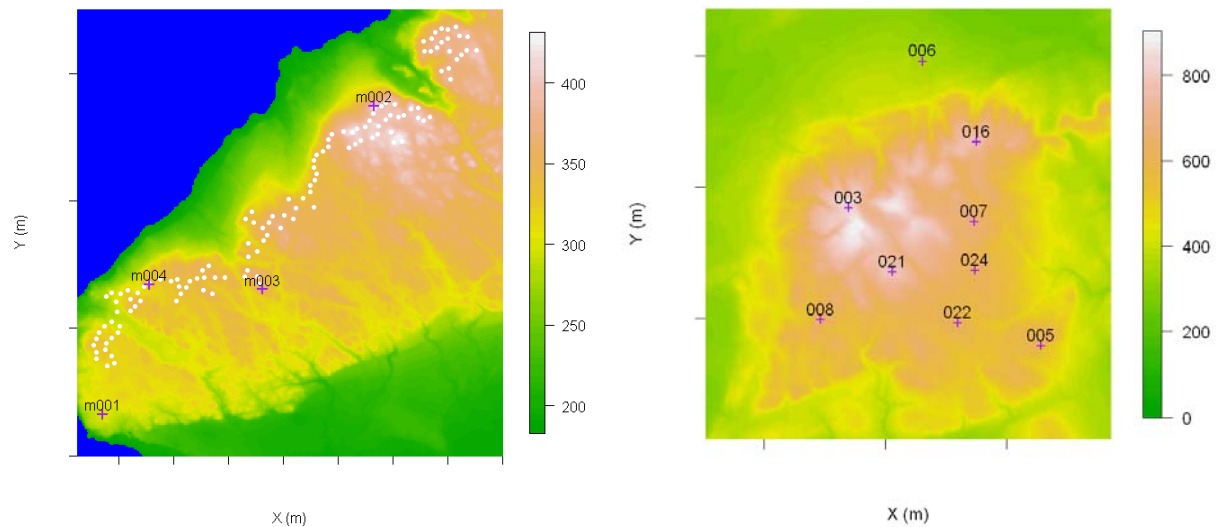


Figure 1. Terrain elevation with met mast locations at the four sites. Site 1 (top left) is fairly flat whereas Site 2 (top right), Site 3 (bottom left) and Site 4 (bottom right) are more complex. The simulation domain was different for each site: 12 km × 17 km for Site 1, 12 km × 12 km for Site 2, and 17 km × 17 km for Site 3 and Site 4.

Computational Fluid Dynamics (CFD) model

The CFD model, Meteodyn WT, developed by Meteodyn, solves the non-linear Navier-Stokes momentum equation with the MIGAL solver (Meteodyn's technical notes). This CFD model assumes an incompressible and steady-state flow and uses a k-l turbulence model based on Yamada (1983) and Arritt (1987). Without solving the conservation of energy equation, the model takes into account the temperature gradient effects through an adjusted turbulence length scale based on thermal stability in the turbulent kinetic energy (TKE) equation. There are 10 different thermal stability classes available in the model but neutral atmospheric conditions were selected as it is the default option. The initial conditions at the inlet are set using the surface roughness, a corresponding reference logarithmic wind speed profile in the surface layer and an Ekman wind speed profile for the remainder of the planetary boundary layer (PBL). In post-processing, the program calculates a directional speed ratio between every point and the mast and applies those ratios to the observed wind speeds. For this study, the program is run with a 50-m grid cell spacing.

Coupled mesoscale NWP and mass-consistent model

The SiteWind system developed at AWS Truepower is composed of the Mesoscale Atmospheric Simulation System (MASS) (Manobianco et al. 1996) and the WindMap mass-consistent diagnostic model (Brower 1999). MASS is a fully compressible, non-hydrostatic NWP model. The mesoscale model is initialized from the NCEP/NCAR reanalysis (Kalnay et al. 1996) dataset and the model is run in cascade mode from a 30-km grid mesh down to 1.2 km (standard SiteWind) or 400 m (high-resolution SiteWind). The PBL scheme implemented in MASS is based on Therry and LaCarrère (1983). The mean wind flow modeled by the mesoscale model is downscaled to 50-m grid spacing using a simple mass-consistent model, WindMap, and high-resolution terrain and land use data sets (Brower et al. 2004).

Coupled mesoscale NWP and LES model

The mesoscale NWP and LES model is the Advanced Regional Prediction System (ARPS) developed at Oklahoma University (Xue et al. 2000). Given sufficient computing power and with the proper choice of grid resolution and sub-grid scale turbulence parameterization scheme, ARPS is equivalent to a LES code. The PBL parameterization scheme in ARPS follows Sun and Chang (1986) and the sub-grid-scale turbulence scheme is based on Moeng (1984) and Deardorff (1980). In this study, ARPS is initialized from the North American

Mesoscale (NAM) model analyses and the ARPS simulations are conducted at resolutions ranging from 12 km down to 90 m. In LES modeling, a rule of thumb is that 80% of the TKE should be resolved explicitly. Figure 2 shows that the 90-m ARPS simulations seem to lie quite close to the inertial sub-range of the 3D turbulent flow observed by a tall tower on site and confirmed by Kolmogorov's 5/3 law. We run ARPS at a final horizontal grid spacing of 90 m to keep the computational burden manageable on two nodes (16 cores) for each 36-hour simulation. This is also the resolution of the surface characteristic databases presently implemented in ARPS.

Runtime

Table 1 compares the runtime of each numerical model for a 12 km × 12 km domain. Typically, there are 3 to 15 meteorological towers installed at a site. The steady-state models (mass-consistent, Jackson-Hunt and CFD) are set up to run over 12 direction sectors (each 30° wide). In addition, the Jackson-Hunt model must be run separately for each mast. The NWP models (both MASS and ARPS) are run for 72 representative 24-hour days with a 12-hour spin-up before the start of each day. Because the NWP model runs are performed on a Linux cluster with as many as 80 dual quad-core nodes, the lapsed clock time is much less than shown - typically less than one day for the NWP model at 1.2 km resolution and 2-3 days for the NWP/LES model at 90 m resolution.

Table 1. Approximate run times in cpu- or core-hours for the different numerical models for a typical 12 km × 12 km domain with 8 masts. The NWP models are run in parallel on a Linux cluster, all others are run on a PC. The NWP models are run for 72 representative 24-hour days. The mass-consistent, Jackson-Hunt and CFD models are run over 12 direction sectors.

Model (resolution)	Jackson-Hunt (50 m)*	CFD (50 m)*	Mass-consistent (50m)#	NWP/mass-consistent (1.2 km/50 m) [§]	NWP/mass-consistent (400 m/50 m) [§]	NWP/LES (90 m) [§]
Time	8	2.5	~1/5	12	32	260
Unit	per mast	per direction	per mast	per day	per day	per day
Total Time	48	30	<2	864	2304	18720

*standard PC → 1 CPU @ 2.50 GHz, 6 GB of RAM

[§] Linux cluster → 1 core @ 2.66 GHz, 16 GB of RAM per nodes

multithreaded on a single CPU 6 core i7 desktop @3.2GHz. 24GB of RAM

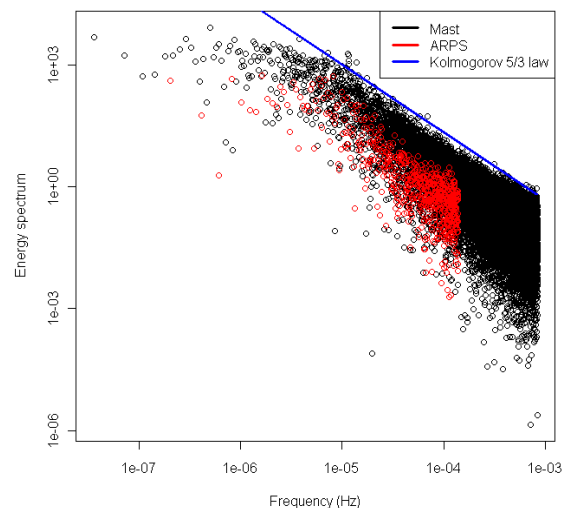


Figure 2. Modeled and observed energy spectrum as a function of frequency at 80 m height (log-log scale) for one of the sites in this study. The 10-minute data from the mast (black points) span a full year, whereas the hourly ARPS data span a sample of 36 days. The blue line is Kolmogorov's 5/3 law.

Metrics of error

The metrics of error for each site are the mean bias and the root mean square error (RMSE) between the predicted and observed mean wind speeds, as defined below:

$$Bias = \frac{1}{N \cdot (N-1)} \sum_{i=1}^N \sum_{\substack{j=1, \\ j \neq i}}^N \left(U_{i,j} - U_i^{obs} \right) \quad (1)$$

$$RMSE = \sqrt{\frac{1}{N \cdot (N-1)} \sum_{i=1}^N \sum_{\substack{j=1, \\ j \neq i}}^N \left(U_{i,j} - U_i^{obs} \right)^2} \quad (2)$$

where N is the number of mast and $U_{i,j}$ is the predicted wind speed at mast i based on the reference mast j and

U_i^{obs} is the observed speed at mast i .

RESULTS AND DISCUSSION

Local near-surface wind climates

Site 1 has gently rolling hills covered with grass and some patchy forest. The wind comes mainly from the south and south-southeast. Although this is apparently a simple site, Figure 3 shows that the wind speeds (at 80 m) and wind shears (below 80 m) are significantly higher at night, reflecting frequent nocturnal low-level jets (LLJ) due to the decoupling of the planetary boundary layer (PBL) after sunset (Rife et al. 2010). A nocturnal LLJ is a thin layer of high wind speeds above the surface layer. The wind maxima are typically found within the first few hundred meters above the ground (> 100 m), but the LLJs nevertheless increase the wind speed at 80 m height as well. High wind shears are also a characteristic of stable layers. Even in the high wind speed range (>10 m/s), the wind shear is not constant and decreases from 0.22 to 0.12. If the atmosphere were mostly in a thermally neutral state, the wind shear would be constant in the high wind speed range due to enhanced mixing.

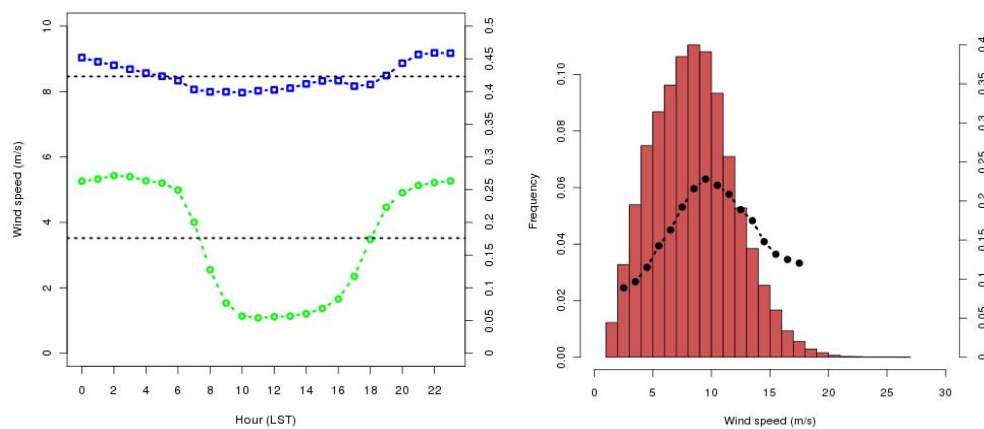


Figure 3. Left: Diurnal wind speed pattern (blue) at 80 m height and wind shear pattern (green) below 80 m observed at a mast at Site 1. Right: Wind speed distribution (red) and mean wind shear exponent (black) by speed for the same mast.

Analyses similar to that shown in Figure 3 were performed for the other sites. Site 2 is located in complex terrain and the land cover is homogeneous grassland. In this case the diurnal wind speed profiles vary significantly but quite the opposite from Site 1. At one mast the wind speeds are stronger during the daytime when the wind shear exponent is low (~ 0.07) and relatively weaker at night when the shear is moderate (~ 0.15). A reasonable explanation is that solar heating induces daytime convection which forces high momentum middle level air to be carried down to the surface. Site 3, which is located near one the Great Lakes in Canada, has a very complex wind climate due to land-lake mesoscale circulations, complex orography, and forest. The prevailing wind directions vary but are generally east-southeast and northwest, i.e., approximately perpendicular to the coastline (Fig. 1, bottom left panel). The diurnal wind speeds and wind shears follow a similar pattern as in Figure 3. However, the mean wind shear exponents average about 0.25 during the day and 0.35 during the night. From a visual inspection of the wind speed and potential temperature profiles predicted by the mesoscale model MASS, nocturnal low-level jets seem to occur somewhat frequently. High wind shear values are also typical of forested areas. Finally, Site 4 is another complex site mostly covered by trees. Its location in the Gaspé Peninsula (Canada) puts it on the track of many winter storms. According to measurements, there is not much diurnal wind speed variation, but the mean wind shear varies from 0.35 in daytime to 0.45 in nighttime.

Validation: error statistics

Each numerical model is run using its default options. The simulations demonstrate that the mesoscale NWP model alone is able to capture the areas of relatively higher and lower wind speeds but the coarse horizontal resolution of the model (1.2 km or 400 m) produces an overly smooth result. The advantage of using a coupled mesoscale NWP model with a mass-consistent model is that the latter is able to capture the fine details of the orography and surface roughness. Another research study (Frank et al., 2001) demonstrated that a coupled mesoscale NWP and microscale model shows improvement over a mesoscale model alone. Upon visual inspection, all numerical models tested in this study exhibit realistic wind flow patterns with lower winds in the valleys and higher winds at the top of the hills and escarpments, as is usually expected.

For each model and each site, the mean wind speed at every mast is predicted from one reference mast at a time using directional speed-up ratios, the standard method for wind plant production studies. The error statistics - the mean bias and RMSE - are calculated from equations (1) and (2). The results for the RMSE are shown in Table 2. The coupled mesoscale NWP-mass-consistent model, SiteWind, performed about as well as the coupled mesoscale NWP-LES model, ARPS. Overall, we did not see much improvement in running the mesoscale NWP model MASS at a higher resolution of 400 m compared to the default 1.2 km. Most importantly, all three coupled NWP models exhibited better accuracy than the Jackson-Hunt and CFD models.

CONCLUSION

The superior performance of all three coupled NWP models suggests that the correct simulation of thermal stability effects and other phenomena related to temperature (and moisture) gradients developed in dynamic mesoscale simulations are of importance in understanding atmospheric wind flow even over domains of quite modest size, such as those studied here. The disadvantage of these approaches is the greater computer power required, especially for the coupled NWP-LES methods. It is up to the user to decide whether the gain in accuracy obtained through these methods is worth the additional cost in computer time (see Table 1).

Table 2. Validation of the modeled mean wind speeds at 80 m a.g.l. using the RMSE calculation from equation (2).

	Site				
	1	2	3	4	Combined
Terrain	Flat	Complex	Complex	Complex	
Land Cover	Mixed	Open	Forested	Forested	
Number of Masts	8	6	3*	9	26

Mean Distance Between Masts	7.3 km	5.0 km	5.7 km	6.0 km	
	RMSE (m/s)				
Linear Jackson-Hunt model	0.26	0.34	1.15	0.74	0.62
CFD model	0.50	0.46	1.07	0.95	0.76
Mass-consistent model	0.32	0.26	0.75	0.76	0.56
Coupled NWP and mass-consistent model	0.10	0.39	0.56	0.67	0.48
Coupled high-res NWP and mass-consistent model	0.24	0.30	0.59	0.63	0.46
NWP/LES model	0.28	0.49	0.57	0.49	0.45

*For Site 3, the simulation domain was too small to include mast 2.

- Overall, the more sophisticated models do perform better at the four sites studied:
 - The coupled mesoscale NWP-mass-consistent model, SiteWind, performed about as well as the coupled NWP-LES model, ARPS. However, the NWP-LES model was run at a significantly lower resolution than the others (90 m compared to 50 m). It is possible that improved accuracy could be obtained at a higher resolution and with further refinements in the turbulence closure and other aspects of this model.
 - The linear microscale model and non-linear CFD model assuming neutral atmospheric conditions produce significantly higher errors. Those models were not designed to fully capture temperature (and moisture) gradient effects. The high performance of the coupled mesoscale NWP-mass-consistent model, SiteWind, suggests that coupling a mesoscale NWP model with the linear microscale model or the CFD model would yield more accurate wind flow estimates than using these two models in a stand-alone mode.
- On-site met mast measurements show that thermal effects have a significant impact on the diurnal cycle and distribution of wind speeds and wind shears:
 - The PBL is rarely in near-neutral conditions except when the winds are moderate to strong with a cloudy sky or around sunrise and sunset.
 - The PBL is rarely in equilibrium
- Pay attention to the local wind climate and mesoscale circulations.
- Know the advantages and limitations of your numerical model.

ACKNOWLEDGEMENTS

We would like to thank the following colleagues at AWS Truepower for their help in this research: Eddie Natenberg, Chuck Alonge, Jeff Freedman, Jeremy Tensen and Colin Rickert. The help of the ARPS support group is also gratefully acknowledged.

REFERENCES

- Artritt, R.W. (1987). "The Effect of water surface boundary layers". *Boundary-layer Meteor.*, vol. 40, pp. 101-125.
- Ayotte, K.W., P.A. Taylor (1995). "A Mixed Spectral Finite-Difference 3D Model of Neutral Planetary Boundary-Layer Flow over Topography". *J. Atmos. Sci.*, vol. 52, pp. 3523-3537.
- Berge, E., A.R. Gravdahl, J. Schelling, L. Tallhaug and O. Undheim (2006). "Wind in complex terrain. A comparison of WASP and two CFD-models". *Proceedings from EWEC 2006*. Athens, Greece.
- Biatsuamlak, G. T. , T. Stathopoulos, and C. Bédard (2004). "Numerical Evaluation of Wind Flow over Complex Terrain: Review". *J. Aerosp. Engrg.* vol. 17, Issue 4, pp. 135-145.
- Brower, M. (1999). "Validation of the WindMap Program and Development of MesoMap". *Proceeding from AWEA's WindPower conference*. Washington, DC, USA.
- Brower, M., J.W. Zack, B. Bailey, M.N. Schwartz and D.L. Elliot (2004). "Mesoscale modeling as a tool for wind resource assessment and mapping". *Proceeding from the American Meteorological Society conference*. Seattle, WA, USA.
- Deardorff, J.W. (1972). "Numerical investigation of neutral and unstable planetary boundary layers". *J. Atmos. Sci.*, vol. 29, pp. 91-115.
- Deardorff, J.W. (1980). "Stratocumulus-capped mixed layers derived from a three-dimensional model". *Bound.-Layer Meteor.*, vol. 18, pp. 495-527.
- Frank, H.P. and L. Landbergh (1997). "Modeling the wind climate of Ireland". *Boundary Layer Meteorology*, vol. 85, pp. 359-378.
- Frank, H.P., O. Rathman, N.G. Mortensen and L. Landberg (2001). "The numerical wind atlas - the KAMM/WASP method". *Report from the Risoe DTU National Laboratory, Roskilde, Denmark*. 59 pp.
- Hale, E., L. Fusina, M. Brower (2011). "Correction Factors For NRG #40 Anemometers Potentially Affected by Dry Friction Whip". *Submitted to the Wind Energy journal*.
- Jackson, P.S. and J.C.R. Hunt (1975). "Turbulent Wind Flow over Low Hill". *Quart. J. R. Met. Soc.*, vol. 101, pp. 929-955.
- Kalnay, E., M. Kanamitsu, R. Kistler, W. Collins, D. Deaven, L. Gandin, M. Iredell, S. Saha, G. White, J. Woollen, Y. Zhu, A. Leetmaa, B. Reynolds, M. Chelliah, W. Ebisuzaki, W. Higgins, J. Janowiak, K. Mo, C. Ropelewski, J. Wang, R. Jenne, et D. Joseph. (1996). "The NCEP-NCAR 40-year reanalysis project". *Bulletin of the American Meteorological Society*, Vol. 77, no. 3, pp. 437-471
- Manobianco, J., J. W. Zack and G.E. Taylor (1996). "Workstation-based real-time mesoscale modeling designed for weather support to operations at the Kennedy Space Center and Cape Canaveral Air Station". *Bull. Amer. Meteor. Soc.*, vol. 77, pp. 653-672.
- Mason P.J. (1994). "Large-eddy simulation: a critical review of the technique". *Quart. J. R. Met. Soc.*, vol. 120, pp. 1-26.
- Meteodyn. "Technical Note - Meteodyn WT version 2.2". *Report from Meteodyn*. Nantes, France. 13 pp.
- Mortensen, N.G, A. J. Bowen, I. Antoniou (2008). "Improving WASP predictions in (too) complex terrain". *Proceedings from EWEC 2008*. Brussels, Belgium.
- Moeng, C-H. and J.C. Wyngaard (1984). "Statistics of conservative scalars in the convective boundary layer". *J. Atmos. Sci.*, vol. 41, pp. 3161-3169.
- Periera, R., R. Guedes, C.S. Santos (2010). "Comparing WASP and CFD wind resource estimates for the "regular" user". *Proceedings from EWEC 2010*. Warsaw, Poland.
- Phillips, G.T. (1979). "A preliminary user's guide for the NOABL objective analysis code". *Report from Science Applications, Inc*. La Jolla, California, USA.
- Reed, R., M. Brower, and J. Kreiselman (2004). "Comparing SiteWind with standard models for energy output estimation". *Proceedings from EWEC*, London, UK.
- Rife, D.L., J.O. Pinto, A.J. Monaghan, C.A. Davis, J.R. Hannan (2010). "Global Distribution and Characteristics of Diurnally Varying Low-Level Jets". *J. of Climate*, vol. 23, pp. 5041-6

- Scire, J.S., F.R. Robe, M.E. Fernau, and R.J. Yamartino (2000). "A user's guide for the CALMET meteorological model (version 5)". Report from Earth Tech, Inc., Concord, Massachusetts, USA. 332 pp.
- Sherman, C. A., (1978). "A mass-consistent model for wind fields over complex terrain". *Journal of Applied Meteorology*, vol. 17, pp. 312-319.
- Sumner, J., C. Sibuet Watters and C. Masson (2010). "CFD in wind energy: the virtual, multiscale wind tunnel". *Energies*, vol. 3, pp. 989-1013.
- Sun, W-Y., and C-Z. Chang (1986). "Diffusion model for a convective layer. Part I: Numerical simulation of convective boundary layer". *J. Clim. Appl. Meteor.*, vol. 25, pp. 1445-1453.
- Taylor, P.A., J.L.Walmsley, J.R. Salmon (1983). "A Simple Model of Neutrally Stratified Boundary-Layer Flow over Real Terrain Incorporating Wave Number-Dependent Scaling". *Boundary-Layer Meteorol.*, vol. 26, pp. 169-189.
- Therry, G. and P. Laccarrère (1983). "Improving the eddy kinetic energy model for planetary boundary layer description", *Bound.-Layer Meteor.*, vol. 25, pp. 63-88.
- Troen, I. (1990). "A High Resolution Spectral Model for Flow in Complex Terrain". Proceedings from the 9th Symposium on Turbulence and Diffusion, Roskilde, Denmark.
- VanLuvanee, D., T. Rogers, G. Randall, A. Williamson, and T. Miller (2009). "Comparison of WAsP, MS-Micro/3, CFD, NWP, and Analytical Methods for Estimating Site-Wide Wind Speeds". Presentation from AWEA Wind Resource Assessment Workshop. Minneapolis, MN.
- Xue, M., K. K. Droegemeier, and V. Wong (2000). "The Advanced Regional Prediction System (ARPS) - A multiscale nonhydrostatic atmospheric simulation and prediction tool. Part I: Model dynamics and verification". *Meteor. Atmos. Physics.*, vol. 75, pp. 161-193.
- Xue, M., K. K. Droegemeier, V. Wong, A. Shapiro, K. Brewster, F. Carr, D. Weber, Y. Liu, and D. Wang (2001). "The Advanced Regional Prediction System (ARPS) - A multiscale nonhydrostatic atmospheric simulation and prediction tool. Part II: Model physics and applications". *Meteor. Atmos. Physics.*, vol. 76, pp. 143- 165.
- Yamada, T. (1983). "Simulations of nocturnal drainage flows by a q^2 turbulence closure model". *J. Atmos. Sci.*, vol. 40, pp. 91-106.